Rare Z-decay into light CP-odd Higgs bosons: a comparative study in different new physics models

Junjie Cao[1], Zhaoxia Heng[2], Jin Min Yang[2]

[1] *Department of Physics, Henan Normal University, Xinxiang 453007, China*

[2] *Key Laboratory of Frontiers in Theoretical Physics, Institute of Theoretical Physics, Academia Sinica, Beijing 100190, China*

Abstract

Various new physics models predict a light CP-odd Higgs boson (labeled as a) and open up new decay modes for Z-boson, such as $Z \to \bar{f}fa$, $Z \to a\gamma$ and $Z \to aaa$, which could be explored at the GigaZ option of the ILC. In this work we investigate these rare decays in several new physics models, namely the type-II two Higgs doublet model (type-II 2HDM), the lepton-specific two Higgs doublet model (L2HDM), the nearly minimal supersymetric standard model (nMSSM) and the next-to-minimal supersymmetric standard model (NMSSM). We find that in the parameter space allowed by current experiments, the branching ratios can reach 10^{-4} for $Z \to \bar{f}fa$ ($f = b, \tau$), 10^{-9} for $Z \to a\gamma$ and 10^{-3} for $Z \to aaa$, which implies that the decays $Z \to \bar{f}fa$ and $Z \to aaa$ may be accessible at the GigaZ option. Moreover, since different models predict different patterns of the branching ratios, the measurement of these rare decays at the GigaZ may be utilized to distinguish the models.

PACS numbers: 13.38.Dg,12.60.Fr,14.80.Da

I. INTRODUCTION

The LEP experiments at the resonance of Z-boson have tested the Standard Model (SM) at quantum level, measuring the Z-decay into fermion pairs with an accuracy of one part in ten thousands. The good agreement of the LEP data with the SM predictions have severely constrained the behavior of new physics at the Z-pole. Taking these achievements into account one can imagine that the physics of Z-boson will again play the central role in the frontier of particle physics if the next generation Z factory comes true with the generated Z events several orders of magnitude higher than that of the LEP. This factory can be realized in the GigaZ option of the International Linear Collider (ILC)[1]. The ILC is a proposed electron-positron collider with tunable energy ranging from 400GeV to 500GeV and polarized beams in its first phase, and the GigaZ option corresponds to its operation on top of the resonance of Z boson by adding a bypass to its main beam line. Given the high luminosity, $\mathcal{L} = 7 \times 10^{33} cm^{-2} s^{-1}$, and the cross section at the resonance of Z boson, $\sigma_Z \simeq 30$nb, about 2×10^9 Z events can be generated in an operational year of $10^7 s$ of GigaZ, which implies that the expected sensitivity to the branching ratio of Z-decay can be improved from 10^{-5} at the LEP to 10^{-8} at the GigaZ[1]. In light of this, the Z-boson properties, especially its exotic or rare decays which are widely believed to be sensitive to new physics, should be investigated comprehensively to evaluate their potential in probing new physics.

Among the rare Z-decays, the flavor changing (FC) processes were most extensively studied to explore the flavor texture in new physics [2], and it was found that, although these processes are severely suppressed in the SM, their branching ratios in new physics models can be greatly enhanced to 10^{-8} for lepton flavor violation decays [3] and 10^{-6} for quark flavor violation decays [4]. Besides the FC processes, the Z-decay into light Higgs boson(s) is another type of rare process that was widely studied, e.g. the decay $Z \to \bar{f} f a$ $(f = b, \tau)$ with the particle a denoting a light Higgs boson was studied in [5], the decay $Z \to a\gamma$ was studied in the two Higgs doublet model (2HDM)[6] and the minimal supersymmetric standard model (MSSM)[7], and the decay $Z \to aaa$ was studied in a model independent way [8], in 2HDM[9, 10] and also in MSSM[11]. These studies indicate that, in contrast with the kinematic forbidden of these decays in the SM, the rates of these decays can be as large as 10^{-5} in new physics models, which lie within the expected sensitivity of the

GigaZ. In this work, we extend the previous studies of these decays to some new models and investigate these decays altogether. We are motivated by some recent studies on the singlet extension of the MSSM, such as the next-to-minimal supersymmetric standard model (NMSSM) [12, 13] and the nearly minimal supersymmetric standard model (nMSSM) [14], where a light CP-odd Higgs boson a with singlet-dominant component may naturally arise from the spontaneous breaking of some approximate global symmetry like $U_R(1)$ or Peccei-Quuin symmetry [15–17]. These non-minimal supersymmetric models can not only avoid the μ-problem, but also alleviate the little hierarchy by having such a light Higgs boson a [18]. We are also motivated by that, with the latest experiments, the properties of the light Higgs boson are more stringently constrained than before. So it is worth updating the previous studies.

So far there is no model-independent lower bound on the lightest Higgs boson mass. In the SM, it must be heavier than 114 GeV, obtained from the null observation of the Higgs boson at LEP experiments. However, due to the more complex structure of the Higgs sector in the extensions of the SM, this lower bound can be significantly relaxed according to recent studies, e.g., for the CP-odd Higgs boson a we have $m_a \gtrsim 1$ GeV in the nMSSM [19], $m_a \gtrsim 0.21$ GeV in the NMSSM [16], and $m_a \gtrsim 7$ GeV in the lepton-specific 2HDM (L2HDM) [20]. With such a light CP-odd Higgs boson, the Z-decay into one or more a is open up. Noting that the decay $Z \to aa$ is forbidden due to Bose symmetry, we in this work study the rare Z-decays $Z \to \bar{f}fa$ $(f = b, \tau)$, $Z \to a\gamma$ and $Z \to aaa$ in a comparative way for four models, namely the Type-II 2HDM[21], the L2HDM [22, 23], the nMSSM and the NMSSM. In our study, we examine carefully the constraints on the light a from many latest experimental results.

This work is organized as follows. In Sec. II we briefly describe the four new physics models. In Sec. III we present the calculations of the rare Z-decays. In Sec. IV we list the constraints on the four new physics models. In Sec. V we show the numerical results for the branching ratios of the rare Z-decays in various models. Finally, the conclusion is given in Sec. VI.

II. THE NEW PHYSICS MODELS

As the most economical way, the SM utilizes one Higgs doublet to break the electroweak symmetry. As a result, the SM predicts only one physical Higgs boson with its properties totally determined by two free parameters. In new physics models, the Higgs sector is usually

extended by adding Higgs doublets and/or singlets, and consequently, more physical Higgs bosons are predicted along with more free parameters involved in.

The general 2HDM contains two $SU(2)_L$ doublet Higgs fields ϕ_1 and ϕ_2, and with the assumption of CP-conserving, its scalar potential can be parameterized as[21]:

$$\begin{aligned} V &= m_1^2\phi_1^\dagger\phi_1 + m_2^2\phi_2^\dagger\phi_2 - (m_3^2\phi_1^\dagger\phi_2 + H.c.) + \frac{\lambda_1}{2}(\phi_1^\dagger\phi_1)^2 + \frac{\lambda_2}{2}(\phi_2^\dagger\phi_2)^2 \\ &+\lambda_3(\phi_1^\dagger\phi_1)(\phi_2^\dagger\phi_2) + \lambda_4(\phi_1^\dagger\phi_2)(\phi_2^\dagger\phi_1) + \frac{\lambda_5}{2}[(\phi_1^\dagger\phi_2)^2 + H.c.], \end{aligned} \tag{1}$$

where λ_i $(i = 1, \cdots, 5)$ are free dimensionless parameters, and m_i $(i = 1, 2, 3)$ are the parameters with mass dimension. After the electroweak symmetry breaking, the spectrum of this Higgs sector includes three massless Goldstone modes, which become the longitudinal modes of $W^\pm$ and Z bosons, and five massive physical states: two CP-even Higgs bosons h_1 and h_2, one neutral CP-odd Higgs particle a and a pair of charged Higgs bosons $H^\pm$. Noting the constraint $v_1^2 + v_2^2 = (246\text{ GeV})^2$ with v_1 and v_2 denoting the vacuum expectation values (vev) of ϕ_1 and ϕ_2 respectively, we choose

$$m_{h_1}, \quad m_{h_2}, \quad m_a, \quad m_{H^\pm}, \quad \tan\beta, \quad \sin\alpha, \quad \lambda_5 \tag{2}$$

as the input parameters with $\tan\beta = v_2/v_1$, and α being the mixing angle that diagonalizes the mass matrix of the CP-even Higgs fields.

The difference between the Type-II 2HDM and the L2HDM comes from the Yukawa coupling of the Higgs bosons to quark/lepton. In the Type-II 2HDM, one Higgs doublet ϕ_2 generates the masses of up-type quarks and the other doublet ϕ_1 generates the masses of down-type quarks and charged leptons; while in the L2HDM one Higgs doublet ϕ_1 couples only to leptons and the other doublet ϕ_2 couples only to quarks. So the Yukawa interactions of a to fermions in these two models are given by [20, 21]

$$\mathcal{L}_{\text{Yukawa}}^{\text{Type-II}} = \frac{igm_{u_i}}{2m_W}\cot\beta\bar{u}_i\gamma^5 u_i a + \frac{igm_{d_i}}{2m_W}\tan\beta\bar{d}_i\gamma^5 d_i a + \frac{igm_{e_i}}{2m_W}\tan\beta\bar{e}_i\gamma^5 e_i a, \tag{3}$$

$$\mathcal{L}_{\text{Yukawa}}^{\text{L2HDM}} = \frac{igm_{u_i}}{2m_W}\cot\beta\bar{u}_i\gamma^5 u_i a - \frac{igm_{d_i}}{2m_W}\cot\beta\bar{d}_i\gamma^5 d_i a + \frac{igm_{e_i}}{2m_W}\tan\beta\bar{e}_i\gamma^5 e_i a, \tag{4}$$

with i denoting generation index. Obviously, in the Type-II 2HDM the $\bar{b}ba$ coupling and the $\bar{\tau}\tau a$ coupling can be simultaneously enhanced by $\tan\beta$, while in the L2HDM only the $\bar{\tau}\tau a$ coupling is enhanced by $\tan\beta$.

The structures of the nMSSM and the NMSSM are described by their superpotentials and corresponding soft-breaking terms, which are given by [24]

$$W_{\rm nMSSM} = W_{\rm MSSM} + \lambda \hat{H}_u \cdot \hat{H}_d \hat{S} + \xi_F M_n^2 \hat{S}, \tag{5}$$

$$W_{\rm NMSSM} = W_{\rm MSSM} + \lambda \hat{H}_u \cdot \hat{H}_d \hat{S} + \frac{1}{3}\kappa \hat{S}^3, \tag{6}$$

$$V_{\rm soft}^{\rm nMSSM} = \tilde{m}_u^2 |H_u|^2 + \tilde{m}_d^2 |H_d|^2 + \tilde{m}_S^2 |S|^2 + (A_\lambda \lambda S H_u \cdot H_d + \xi_S M_n^3 S + h.c.), \tag{7}$$

$$V_{\rm soft}^{\rm NMSSM} = \tilde{m}_u^2 |H_u|^2 + \tilde{m}_d^2 |H_d|^2 + \tilde{m}_S^2 |S|^2 + (A_\lambda \lambda S H_u \cdot H_d + \frac{A_\kappa}{3}\kappa S^3 + h.c.), \tag{8}$$

where $W_{\rm MSSM}$ is the superpotential of the MSSM without the μ term, $\hat{H}_{u,d}$ and $\hat{S}$ are Higgs doublet and singlet superfields with $H_{u,d}$ and S being their scalar component respectively, $\tilde{m}_u$, $\tilde{m}_d$, $\tilde{m}_S$, A_λ, A_κ and $\xi_S M_n^3$ are soft breaking parameters, and λ and κ are coefficients of the Higgs self interactions.

With the superpotentials and the soft-breaking terms, one can get the Higgs potentials of the nMSSM and the NMSSM respectively. Like the 2HDM, the Higgs bosons with same CP property will mix and the mass eigenstates are obtained by diagonalizing the corresponding mass matrices:

$$\begin{pmatrix} h_1 \\ h_2 \\ h_3 \end{pmatrix} = U^H \begin{pmatrix} \phi_u \\ \phi_d \\ \sigma \end{pmatrix}, \quad \begin{pmatrix} a \\ A \\ G^0 \end{pmatrix} = U^A \begin{pmatrix} \varphi_u \\ \varphi_d \\ \xi \end{pmatrix}, \quad \begin{pmatrix} H^+ \\ G^+ \end{pmatrix} = U \begin{pmatrix} H_u^+ \\ H_d^+ \end{pmatrix}, \tag{9}$$

where the fields on the right hands of the equations are component fields of H_u, H_d and S defined by

$$H_d = \begin{pmatrix} \frac{v_d+\phi_d+i\varphi_d}{\sqrt{2}} \\ H_d^- \end{pmatrix}, \quad H_u = \begin{pmatrix} H_u^+ \\ \frac{v_u+\phi_u+i\varphi_u}{\sqrt{2}} \end{pmatrix}, \quad S = \frac{1}{\sqrt{2}}\left(s+\sigma+i\xi\right), \tag{10}$$

h_1, h_2, h_3 and a, A are respectively the CP-even and CP-odd neutral Higgs bosons, G^0 and G^+ are Goldstone bosons eaten by Z and W^+, and H^+ is the charged Higgs boson. So both the nMSSM and NMSSM predict three CP-even Higgs bosons, two CP-odd Higgs bosons and one pair of charged Higgs bosons. In general, the lighter CP-odd Higgs a in these model is the mixture of the singlet field ξ and the doublet field combination, $\cos\beta\varphi_u + \sin\beta\varphi_d$, i.e.

$$a = \cos\theta_A \xi + \sin\theta_A(\cos\beta\varphi_u + \sin\beta\varphi_d), \tag{11}$$

and its couplings to down-type quarks are then proportional to $\frac{gm_q}{m_W}\tan\beta\sin\theta_A$. So for singlet dominated a, $\sin\theta_A$ is small and the couplings are suppressed. As a comparison, the

interactions of a with the squarks are given by[12]

$$\begin{aligned}\mathcal{L}_{a\tilde{q}^*\tilde{q}} &= \frac{-igm_u}{2m_W}\left(\lambda v\cot\beta\cos\theta_A + A_u\cot\beta\sin\theta_A - \mu\sin\theta_A\right)(\tilde{u}_R^*\tilde{u}_L - \tilde{u}_L^*\tilde{u}_R)a \\ &\quad -\frac{igm_d}{2m_W}\left(\lambda v\tan\beta\cos\theta_A + A_d\tan\beta\sin\theta_A - \mu\sin\theta_A\right)(\tilde{d}_R^*\tilde{d}_L - \tilde{d}_L^*\tilde{d}_R)a, \qquad (12)\end{aligned}$$

i.e. the interaction does not vanish when $\sin\theta_A$ approaches zero. Just like the 2HDM where we use the vevs of the Higgs fields as fundamental parameters, we choose λ, κ, $\tan\beta$, $\mu_{eff} = \lambda\langle S\rangle$, A_κ and $m_A^2 = \frac{2\mu}{\sin 2\beta}(A_\lambda + \frac{\kappa\mu}{\lambda})$ as input parameters for the NMSSM[24] and λ, $\tan\beta$, $\mu_{eff} = \lambda\langle S\rangle$, A_λ, $\tilde{m}_S$ and $m_A^2 = \frac{2}{\sin 2\beta}(\mu A_\lambda + \lambda\xi_F M_n^2)$ as input parameters for the nMSSM[19].

About the nMSSM and the NMSSM, three points should be noted. The first is for the two models, there is no explicit $\mu-$term, and the effective μ parameter ($\mu_{\rm eff}$) is generated when the scalar component of $\hat{S}$ develops a vev. The second is, the nMSSM is actually same as the NMSSM with $\kappa = 0$[19], because the tadpole terms $\xi_F M_n^2\hat{S}$ and its soft breaking term $\xi_S M_n^3 S$ in the nMSSM do not induce any interactions, except for the tree-level Higgs boson masses and the minimization conditions. And the last is despite of the similarities, the nMSSM has its own peculiarity, which comes from its neutralino sector. In the basis $(-i\lambda', -i\lambda^3, \psi_{H_u}^0, \psi_{H_d}^0, \psi_S)$, its neutralino mass matrix is given by [14]

$$\begin{pmatrix} M_1 & 0 & m_Z s_W s_b & -m_Z s_W c_b & 0 \\ 0 & M_2 & -m_Z c_W s_b & m_Z c_W c_b & 0 \\ m_Z s_W s_b & -m_Z c_W s_b & 0 & -\mu & -\lambda v c_b \\ -m_Z s_W c_b & m_Z c_W c_b & -\mu & 0 & -\lambda v s_b \\ 0 & 0 & -\lambda v c_b & -\lambda v s_b & 0 \end{pmatrix} \qquad (13)$$

where M_1 and M_2 are $U(1)$ and $SU(2)$ gaugino masses respectively, $s_W = \sin\theta_W$, $c_W = \cos\theta_W$, $s_b = \sin\beta$ and $c_b = \cos\beta$. After diagonalizing this matrix one can get the mass eigenstate of the lightest neutralino $\tilde{\chi}_1^0$ with mass taking the following form [25]

$$m_{\tilde{\chi}_1^0} \simeq \frac{2\mu\lambda^2(v_u^2+v_d^2)}{2\mu^2+\lambda^2(v_u^2+v_d^2)}\frac{\tan\beta}{\tan^2\beta+1} \qquad (14)$$

This expression implies that $\tilde{\chi}_1^0$ must be lighter than about 60 GeV for $\mu > 100$GeV (from lower bound on chargnio mass) and $\lambda < 0.7$ (perturbativity bound). Like the other supersymmetric models, $\tilde{\chi}_1^0$ as the lightest sparticle acts as the dark matter in the universe, but due to its singlino-dominated nature, it is difficult to annihilate sufficiently to get the correct

density in the current universe. So the relic density of $\tilde{\chi}_1^0$ plays a crucial way in selecting the model parameters. For example, as shown in [19], for $\tilde{\chi}_1^0 > 37\text{GeV}$, there is no way to get the correct relic density, and for the other cases, $\tilde{\chi}_1^0$ mainly annihilates by exchanging Z boson for $30\text{GeV} < m_{\tilde{\chi}_1^0} < 37\text{GeV}$, or by exchanging a light CP-odd Higgs boson a with mass satisfying the relation $m_a \simeq 2m_{\tilde{\chi}_1^0}$ for $m_{\tilde{\chi}_1^0} < 25\text{GeV}$. For the annihilation, $\tan\beta$ and μ are required to be less than 10 and 500GeV respectively because through Eq.(14) a large $\tan\beta$ or μ will suppress $m_{\tilde{\chi}_1^0}$ to make the annihilation more difficult. The properties of the lightest CP-odd Higgs boson a, such as its mass and couplings, are also limited tightly since a plays an important role in $\tilde{\chi}_1^0$ annihilation. The phenomenology of the nMSSM is also rather special, and this was discussed in detail in [19].

III. CALCULATIONS

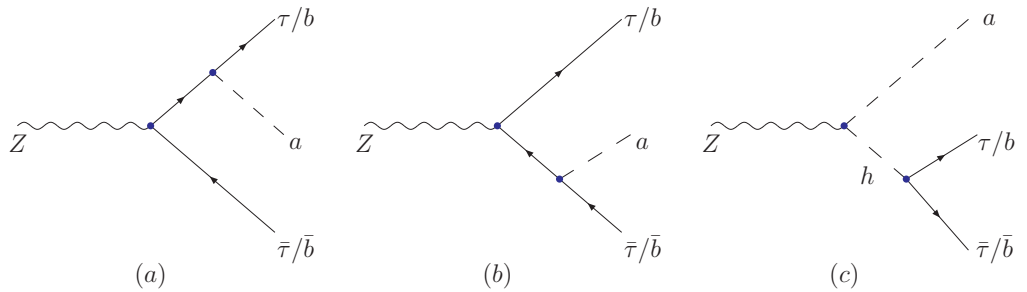

FIG. 1: Feynman diagrams contributing to the decay $Z \to \bar{f}fa$ $(f = b, \tau)$ in new physics models. h denotes all possible intermediate CP-even Higgs bosons in the corresponding model.

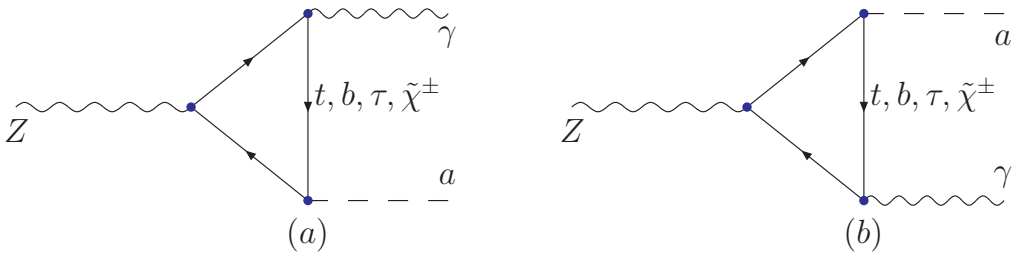

FIG. 2: Feynman diagrams contributing to the decay $Z \to a\gamma$ at one-loop level in new physics models. Note the chargino loop diagrams only exist in the nMSSM and NMSSM.

In the Type-II 2HDM, L2HDM, nMSSM and NMSSM, the rare Z-decays $Z \to \bar{f}fa$ $(f = b, \tau)$, $Z \to a\gamma$ and $Z \to aaa$ may proceed by the Feynman diagrams shown in Fig.1, Fig.2 and Fig.3 respectively. For these diagrams, the intermediate state h represents all

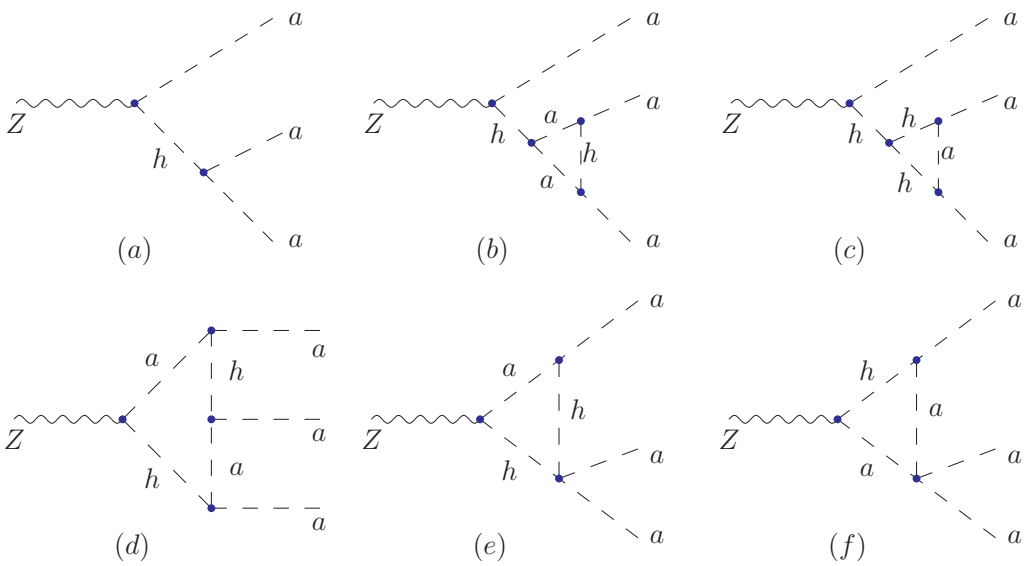

FIG. 3: Feynman diagrams contributing to the decay $Z \to aaa$ in new physics models. Only the correction from the Higgs-mediated loops are considered since the other corrections can be safely neglected (see the arguments in the text).

possible CP-even Higgs bosons in the corresponding model, i.e. h_1 and h_2 in Type-II 2HDM and L2HDM and h_1, h_2 and h_3 in nMSSM and NMSSM. In order to take into account the possible resonance effects of h in Fig.1(c) for $Z \to \bar{f}fa$ and Fig.3 (a) for $Z \to aaa$, we have calculated all the decay modes of h and properly included the width effect in its propagator. As to the decay $Z \to a\gamma$, two points should be noted. One is, unlike the decays $Z \to \bar{f}fa$ and $Z \to aaa$, this process proceeds only through loops mediated by quarks/leptons in the Type-II 2HDM and L2HDM, and additionally by sparticles in the nMSSM and NMSSM. So in most cases its rate should be much smaller than the other two. The other is due to CP-invariance, loops mediated by squarks/sleptons give no contribution to the decay[7]. In actual calculation, this is reflected by the fact that the coupling coefficient of $\tilde{q}_R^* \tilde{q}_L a$ differs from that of $\tilde{q}_L^* \tilde{q}_R a$ by a minus sign (see Eq.(12)), and as a result, the squark-mediated contributions to $Z \to a\gamma$ are completely canceled out.

With regard to the rare decay $Z \to aaa$, we have more explanations. In the lowest order, this decay proceeds by the diagram shown in Fig.3 (a), and hence one may think that, as a rough estimate, it is enough to only consider the contributions from Fig.3(a). However, we note that in some cases of the Type-II 2HDM and L2HDM, due to the cancelation of the contributions from different h in Fig.3 (a) and also due to the potentially

largeness of haa couplings (i.e. larger than the electroweak scale v), the radiative correction from the Higgs-mediated loops may dominate over the tree level contribution even when the tree level prediction of the rate, $Br_{tree}(Z \to aaa)$, exceeds 10^{-6}. On the other hand, we find the contribution from quark/lepton-mediated loops can be safely neglected if $Br_{tree}(Z \to aaa) > 10^{-8}$ in the Type-II 2HDM and the L2HDM. In the nMSSM and the NMSSM, besides the corrections from the Higgs- and quark/lepton-mediated loops, loops involving sparticles such as squarks, charginos and neutralinos can also contribute to the decay. We numerically checked that the contributions from squarks and charginos can be safely neglected if $Br_{tree}(Z \to aaa) > 10^{-8}$. We also calculated part of potentially large neutralino correction (note that there are totally about 5^4 diagrams for such correction!) and found they can be neglected too. Since considering all the radiative corrections will make our numerical calculation rather slow, we only include the most important correction, namely that from Higgs-mediated loops, in presenting our results for the four models.

One can intuitively understand the relative smallness of the sparticle contribution to $Z \to aaa$ as follows. First consider the squark contribution which is induced by the $Z\tilde{q}^*\tilde{q}$ interaction ($\tilde{q}$ denotes the squark in chirality state) and the $\tilde{q}^*\tilde{q}a$ interaction through box diagrams. Because the $Z\tilde{q}^*\tilde{q}$ interaction conserves the chirality of the squarks while the $\tilde{q}^*\tilde{q}a$ interaction violates the chirality, to get non-zero contribution to $Z \to aaa$ from the squark loops, at least four chiral flippings are needed, with three of them provided by $\tilde{q}^*\tilde{q}a$ interaction and the rest provided by the left-right squark mixing. This means that, if one calculates the amplitude in the chirality basis with the mass insertion method, the amplitude is suppressed by the mixing factor $\frac{m_q X_q}{m^2_{\tilde{q}}}$ with $m_q X_q$ being the off diagonal element in squark mass matrix. Next consider the chargino/neutralino contributions. Since for a light a, its doublet component, parameterized by $\sin\theta_A$ in Eq.(11), is usually small, the couplings of a with the sparticles will never be tremendously large[12]. So the chargino/neutralino contributions are not important too. In our calculation of the decays, we work in the mass eigenstates of sparticles instead of in the chirality basis.

IV. CONSTRAINTS ON THE NEW PHYSICS MODELS

For the Type-II 2HDM and the L2HDM, we consider the following constraints [20]:

(1) Theoretical constraints on λ_i from perturbativity, unitarity and requirements that the

scalar potential is finit at large field values and contains no flat directions [21, 26], which imply that

$$\begin{aligned}
&\lambda_i < 4\pi \ (i = 1, 5), \quad \lambda_{1,2} > 0, \quad \lambda_3 > -\sqrt{\lambda_1 \lambda_2}, \quad \lambda_3 + \lambda_4 - |\lambda_5| > -\sqrt{\lambda_1 \lambda_2}, \\
&3(\lambda_1 + \lambda_2) \pm \sqrt{9(\lambda_1 - \lambda_2)^2 + 4(2\lambda_3 + \lambda_4)^2} < 16\pi, \\
&\lambda_1 + \lambda_2 \pm \sqrt{(\lambda_1 - \lambda_2)^2 + 4|\lambda_4|^2} < 16\pi, \\
&\lambda_1 + \lambda_2 \pm \sqrt{(\lambda_1 - \lambda_2)^2 + 4|\lambda_5|^2} < 16\pi, \\
&\lambda_3 + 2\lambda_4 \pm 3|\lambda_5| < 8\pi, \quad \lambda_3 \pm \lambda_4 < 8\pi, \quad \lambda_3 \pm |\lambda_5| < 8\pi. \qquad (15)
\end{aligned}$$

(2) The constraints from the LEP search for neutral Higgs bosons. We compute the signals from the Higgs-strahlung production $e^+e^- \to Zh_i$ $(i = 1, 2)$ with $h_i \to 2b, 2\tau, 4b, 4\tau, 2b2\tau$ [27–29] and from the associated production $e^+e^- \to h_i a$ with $h_i a \to 4b, 4\tau, 2b2\tau, 6b, 6\tau$ [30], and compare them with the corresponding LEP data which have been inputted into our code. We also consider the constraints from $e^+e^- \to Zh_i$ by looking for a peak of M_{h_i} recoil mass distribution of Z-boson [31] and the constraint of $\Gamma(Z \to h_i a) < 5.8$ MeV when $m_a + m_{h_i} < m_Z$ [32].

These constraints limit the quantities such as $C^{2b}_{eff} = [g^2_{ZZh_i}/g^2_{ZZh_{SM}}] \times Br(h_i \to \bar{b}b)$ on the $C^{2b}_{eff} - m_{h_i}$ plane with the the subscript g_{ZZh_i} denoting the coupling coefficient of the ZZh_i interaction. They also impose a model-dependent lower bound on m_{h_i}, e.g., 70GeV for the Type-II 2HDM (from our scan results), 50GeV for the L2HDM[20], and 30GeV for the nMSSM [19]. These bounds are significantly lower than that of the SM, i.e. 114GeV, partially because in new physics models, unconventional decay modes of h_i such as $h_i \to aa$ are open up. As to the nMSSM, another specific reason for allowing a significantly lighter CP-even Higgs boson is that the boson may be singlet-dominated in this model.

With regard to the lightest CP-odd Higgs boson a, we checked that there is no lower bound on its mass so long as the $Zh_i a$ interaction is weak or h_i is sufficiently heavy.

(3) The constraints from the LEP search for a light Higgs boson via the Yukawa process $e^+e^- \to \bar{f}fS$ with $f = b, \tau$ and S denoting a scalar [33]. These constraints can limit the $\bar{f}fS$ coupling versus m_S in new physics models.

(4) The constraints from the CLEO-III limit on $Br(\Upsilon(1S) \to a\gamma \to \tau^+\tau^-\gamma)$ and the latest

BaBar limits on $Br(\Upsilon(3S) \to a\gamma \to \tau^+\tau^-\gamma, \mu^+\mu^-\gamma)$. These constraints will put very tight constraints on the $a\bar{b}b$ coupling for $m_a < 9$GeV. In our analysis, we use the results of Fig.8 in the second paper of [17] to excluded the unfavored points.

(5) The constraints from $Z\tau^+\tau^-$ couplings. Since the Higgs sector can give sizable higher order corrections to $Z\tau^+\tau^-$ couplings, we calculate them to one loop level and require the corrected $Z\tau^+\tau^-$ couplings to lie within the 2σ range of their fitted value. The SM predictions for the couplings at Z-pole are given by $g_V^{SM} = -0.03712$ and $g_A^{SM} = -0.50127$ [34], and the fitted values are given by -0.0366 ± 0.00245 and -0.50204 ± 0.00064, respectively[34]. We adopt the formula in [35] to the 2HDM in our calculation.

(6) The constraints from τ leptonic decay. We require the new physics correction to the branching ratio $Br(\tau \to e\bar{\nu}_e\nu_\tau)$ to be in the range of $-0.80\% \sim 1.21\%$ [36]. We use the formula in [36] in our calculation.

About the constraints (5) and (6), two points should be noted. One is all Higgs bosons are involved in the constraints by entering the self energy of τ lepton, the $Z\bar{\tau}\tau$ vertex correction or the $W\bar{\tau}\nu_\tau$ vertex correction, and also the box diagrams for $\tau \to e\bar{\nu}_e\nu_\tau$[35, 36]. Since the Yukawa couplings of the Higgs bosons to τ lepton get enhanced by $\tan\beta$ and so do the corrections, $\tan\beta$ must be upper bounded for given spectrum of the Higgs sector. Generally speaking, the lighter a is, the more tightly $\tan\beta$ is limited[20, 36]. The other point is in the Type-II 2HDM, R_b, B-physics observables as well as Υ decays discussed above can constraint the model in a tighter way than the constraints (5) and (6) since the Yukawa couplings of τ lepton and b quark are simultaneously enhanced by $\tan\beta$. But for the L2HDM, because only the Yukawa couplings of τ lepton get enhanced (see Eq.4), the constraints (5) and (6) are more important in limiting $\tan\beta$.

(7) Indirect constraints from the precision electroweak observables such as ρ_ℓ, $\sin^2\theta_{eff}^\ell$ and M_W, or their combinations $\epsilon_i (i = 1, 2, 3)$ [37]. We require ϵ_i to be compatible with the LEP/SLD data at 95% confidence level[34]. We also require new physics prediction of $R_b = \Gamma(Z \to \bar{b}b)/\Gamma(Z \to \text{hadrons})$ is within the 2σ range of its experimental value. The latest results for R_b are $R_b^{exp} = 0.21629 \pm 0.00066$ (measured value) and $R_b^{SM} = 0.21578$ (SM prediction) for $m_t = 173$ GeV [38]. In our code, we adopt the

formula for these observables presented in [35] to the Type-II 2HDM and the L2HDM respectively.

In calculating ρ_ℓ, $\sin^2\theta^\ell_{eff}$ and M_W, we note that these observables get dominant contributions from the self energies of the gauge bosons Z, W and γ. Since there is no Zaa coupling or γaa coupling, a must be associated with the other Higgs bosons to contribute to the self energies. So by the UV convergence of these quantities, one can infer that, for the case of a light a and $m_{h_i}, m_{H^\pm} \gg m_Z$, these quantities depend on the spectrum of the Higgs sector in a way like $\ln\frac{m^2_{h_i}}{m^2_{H^\pm}}$ at leading order, which implies that a light a can still survive the constraints from the precision electroweak observables given the splitting between m_{h_i} and $m_{H^\pm}$ is moderate[20].

(8) The constraints from B physics observables such as the branching ratios for $B \to X_s\gamma$, $B_s \to \mu^+\mu^-$ and $B^+ \to \tau^+\nu_\tau$, and the mass differences ΔM_d and ΔM_s. We require their theoretical predications to agree with the corresponding experimental values at 2σ level.

In the Type-II 2HDM and the L2HDM, only the charged Higgs boson contributes to these observables by loops, so one can expect that $m_{H^\pm}$ versus $\tan\beta$ is to be limited. Combined analysis of the limits in the Type-II 2HDM has been done by the CKMfitter Group, and the lower bound of $m_{H^\pm}$ as a function of $\tan\beta$ was given in Fig.11 of [39]. This analysis indicates that $m_{H^\pm}$ must be heavier than 316GeV at 95% C.L. regardless the value of $\tan\beta$. In this work, we use the results of Fig.11 in [39] to exclude the unfavored points. As for the L2HDM, B physics actually can not put any constraints[40] because in this model the couplings of the charged Higgs boson to quarks are proportional to $\cot\beta$ and in the case of large $\tan\beta$ which we are interested in, they are suppressed. In our analysis of the L2HDM, we impose the LEP bound on $m_{H^\pm}$, i.e. $m_{H^\pm} > 92$GeV[41].

(9) The constraints from the muon anomalous magnetic moment a_μ. Now both the theoretical prediction and the experimental measured value of a_μ have reached a remarkable precision, but a significant deviation still exists: $a_\mu^{exp} - a_\mu^{SM} = (25.5 \pm 8.0) \times 10^{-10}$ [42]. In the 2HDM, a_μ gets additional contributions from the one-loop diagrams induced by the Higgs bosons and also from the two-loop Barr-Zee diagrams mediated by a and h_i[43]. If the Higgs bosons are much heavier than μ lepton mass, the contributions

from the Barr-Zee diagrams are more important, and to efficiently alleviate the discrepancy of a_μ, one needs a light a along with its enhanced couplings to μ lepton and also to heavy fermions such as bottom quark and τ lepton to push up the effects of the Barr-Zee diagram[43]. The CP-even Higgs bosons are usually preferred to be heavy since their contributions to a_μ are negative.

In the Type-II 2HDM, because $\tan\beta$ is tightly constrained by the process $e^+e^- \to \bar{b}ba$ at the LEP[33] and the Υ decay[17], the Barr-Zee diagram contribution is insufficient to enhance a_μ to 2σ range around its measured value[44]. So in our analysis, we require the Type-II 2HDM to explain a_μ at 3σ level. While for the L2HDM, $\tan\beta$ is less constrained compared with the Type-II 2HDM, and the Barr-Zee diagram involving the τ-loop is capable to push up greatly the theoretical prediction of a_μ[20]. Therefore, we require the L2HDM to explain the discrepancy at 2σ level.

Unlike the other constraints discussed above, the a_μ constraint will put a two-sided bound on $\tan\beta$ since on the one hand, it needs a large $\tan\beta$ to enhance the Barr-Zee contribution, but on the other hand, too large $\tan\beta$ will result in an unacceptable large a_μ.

(10) Since this paper concentrates on a light a, the decay $h_i \to aa$ is open up with a possible large decay width. We require the width of any Higgs boson to be smaller than its mass to avoid a too fat Higgs boson[10]. We checked that for the scenario characterized by $m_{h_2}/m_{h_1} > 3$, the coefficient of h_iaa interaction is usually larger than the electroweak scale v, and consequently a large decay width is resulted.

For the nMSSM and NMSSM, the above constraints become more complicated because in these models, not only more Higgs bosons are involved in, but also sparticles enter the constraints. So it is not easy to understand some of the constraints intuitively. Take the process $B \to X_s\gamma$ as an example. In the supersymmetric models, besides the charged Higgs contribution, chargino loops, gluino loops as well as neutralino loops also contribute to the process[45], and depending on the SUSY parameters, any of these contributions may become dominated over or be canceled by other contributions. As a result, although the charged Higgs affects the process in the same way as that in the Type-II 2HDM, charged Higgs as light as 130GeV is still allowed even for $\tan\beta > 50$[46].

Since among the constraints, a_μ is rather peculiar in that it needs new physics to explain the discrepancy between a_μ^{exp} and a_μ^{SM}, we discuss more about its dependence on SUSY parameters. In the nMSSM and the NMSSM, a_μ receives contributions from Higgs loops and neutralino/chargino loops. For the Higgs contribution, it is quite similar to that of the Type-II 2HDM except that more Higgs bosons are involved in[47]. For the neutralino/chargino contribution, in the light bino limit (i.e. $M_1 \ll M_2, \mu$), it can be approximated by[48]

$$\delta a_\mu = 18 \tan\beta \left(\frac{100\text{GeV}}{m_{\tilde{\mu}}}\right)^3 \left(\frac{\mu - A_t \cot\beta}{1000\text{GeV}}\right) 10^{-10} \tag{16}$$

for $m_{\tilde{\mu}_1} \simeq m_{\tilde{\mu}_2} = m_{\tilde{\mu}} = 2M_1$ with $m_{\tilde{\mu}_i}$ being smuon mass. So combining the two contributions together, one can learn that a light a along with large $\tan\beta$ and/or light smuon with moderate $\tan\beta$ are favored to dilute the discrepancy.

Because more parameters are involved in the constraints on the supersymmetric models, we consider following additional constraints to further limit their parameters:

(a) Direct bounds on sparticle masses from the LEP1, the LEP2 and the Tevatron experiments [38].

(b) The LEP1 bound on invisible Z decay $\Gamma(Z \to \tilde{\chi}_1^0\tilde{\chi}_1^0) < 1.76$ MeV; the LEP2 bound on neutralino production $\sigma(e^+e^- \to \tilde{\chi}_1^0\tilde{\chi}_i^0) < 10^{-2}$ pb $(i > 1)$ and $\sigma(e^+e^- \to \tilde{\chi}_i^0\tilde{\chi}_j^0) < 10^{-1}$ pb $(i, j > 1)$[49].

(c) Dark matter constraints from the WMAP relic density $0.0975 < \Omega h^2 < 0.1213$ [50].

Note that among the above constraints, the constraint (2) on Higgs sector and the constraint (c) on neutralino sector are very important. This is because in the supersymmetric models, the SM-like Higgs is upper bounded by about 100GeV at tree level and by about 140GeV at loop level, and that the relic density restricts the LSP annihilation cross section in a certain narrow range.

In our analysis of the NMSSM, we calculate the constraints (3) and (5-7) by ourselves and utilize the code NMSSMTools [51] to implement the rest constraints. We also extend NMSSMTools to the nMSSM to implement the constraints. For the extension, the most difficult thing we faced is how to adapt the code micrOMEGAs[52] to the nMSSM case. We solve this problem by noting the following facts:

- As we mentioned before, the nMSSM is actually same as the NMSSM with the trilinear singlet term setting to zero. So we can utilize the model file of the NMSSM as the input of the micrOMEGAs and set $\kappa = 0$.

- Since in the nMSSM, the LSP is too light to annihilate into Higgs pairs, there is no need to reconstruct the effective Higgs potential to calculate precisely the annihilation channel $\chi_1^0\chi_1^0 \to SS$ with S denoting any of Higgs bosons[53].

We thank the authors of the NMSSMTools for helpful discussion on this issue when we finish such extension[19].

V. NUMERICAL RESULTS AND DISCUSSIONS

With the above constraints, we perform four independent random scans over the parameter space of the Type-II 2HDM, the L2HDM, the nMSSM and the NMSSM respectively. We vary the parameters in following ranges:

$$\begin{aligned} 1 \leq \tan\beta \leq 80,\ \ -\sqrt{2}/2 \leq \sin\alpha \leq \sqrt{2}/2,\ m_a \leq 30\ \text{GeV},\ \lambda_5 \leq 4\pi, \\ 5\ \text{GeV} \leq m_{h_1,h_2} \leq 500\ \text{GeV}, \quad 316\ \text{GeV} \leq m_{H^+} \leq 500\ \text{GeV} \end{aligned} \tag{17}$$

for the Type-II 2HDM,

$$\begin{aligned} 1 \leq \tan\beta \leq 80,\ \ -\sqrt{2}/2 \leq \sin\alpha \leq \sqrt{2}/2,\ m_a \leq 30\ \text{GeV},\ \lambda_5 \leq 4\pi, \\ 5\ \text{GeV} \leq m_{h_1,h_2} \leq 500\ \text{GeV}, \quad 92\text{GeV} \leq m_{H^+} \leq 500\ \text{GeV} \end{aligned} \tag{18}$$

for the L2HDM,

$$\begin{aligned} 0.1 \leq \lambda \leq 0.7,\ 1 \leq \tan\beta \leq 80,\ 100\ \text{GeV} \leq m_A \leq 1\ \text{TeV}, \\ 50\ \text{GeV} \leq \mu_{\text{eff}}, M_1 \leq 500\ \text{GeV},\ \ -1\ \text{TeV} \leq A_\lambda \leq 1\ \text{TeV},\ 0 \leq \tilde{m}_S \leq 200\text{GeV} \end{aligned} \tag{19}$$

for the nMSSM, and

$$\begin{aligned} 0.1 \leq \lambda, \kappa \leq 0.7,\ 1 \leq \tan\beta \leq 80,\ 100\ \text{GeV} \leq m_A \leq 1\ \text{TeV}, \\ 50\ \text{GeV} \leq \mu_{\text{eff}}, M_1 \leq 500\ \text{GeV},\ \ -100\ \text{GeV} \leq A_\kappa \leq 100\ \text{GeV} \end{aligned} \tag{20}$$

for the NMSSM.

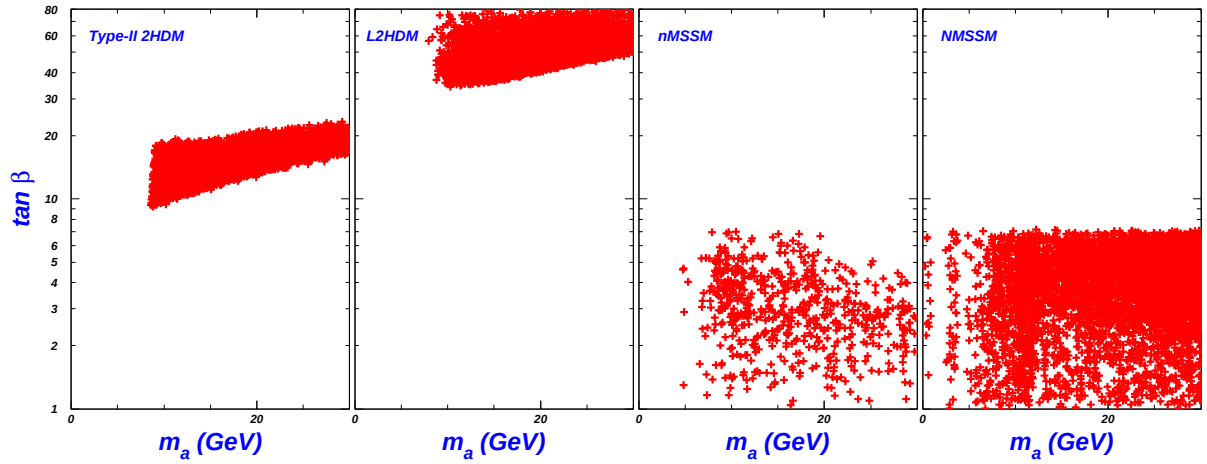

FIG. 4: The scattering plot of the surviving samples projected on $m_a - \tan\beta$ plane.

In performing the scans, we note that for the nMSSM and the NMSSM, some constraints also rely on the gaugino masses and the soft breaking parameters in the squark sector and the slepton sector. Since these parameters affect little on the properties of a, we fix them to reduce the number of free parameters in our scan. For the squark sector, we adopt the m_h^{max} scenario which assumes that the soft mass parameters for the third generation squarks are degenerate: $M_{Q_3} = M_{U_3} = M_{D_3} = 800$ GeV, and that the trilinear couplings of the third generation squarks are also degenerate, $A_t = A_b$ with $X_t = A_t - \mu\cot\beta = -2M_{Q_3}$. For the slepton sector, we assume all the soft-breaking masses and trilinear parameters to be 100 GeV. This setting is necessary for the nMSSM since this model is difficult to explain the muon anomalous moment at 2σ level for heavy sleptons[19]. Finally, we assume the grand unification relation $3M_1/5\alpha_1 = M_2/\alpha_2 = M_3/\alpha_3$ for the gaugino masses with α_i being fine structure constants of the different gauge group.

With large number of random points in the scans, we finally get about 3000, 5000, 800 and 3000 samples for the Type-II 2HDM, the L2HDM, the nMSSM and the NMSSM respectively which survive the constraints and satisfy $m_a \leq 30$GeV. Analyzing the properties of the a indicates that for most of the surviving points in the nMSSM and the NMSSM, its dominant component is the singlet field (numerically speaking, $\cos\theta_A > 0.7$) so that its couplings to the SM fermions are suppressed[15, 19]. Our analysis also indicates that the main decay products of a are $\bar{\tau}\tau$ for the L2HDM[20], $\bar{b}b$ (dominant) and $\bar{\tau}\tau$ (subdominant) for the Type-II 2HDM, the nMSSM and the NMSSM, and in some rare cases, neutralino pairs in the nMSSM[19].

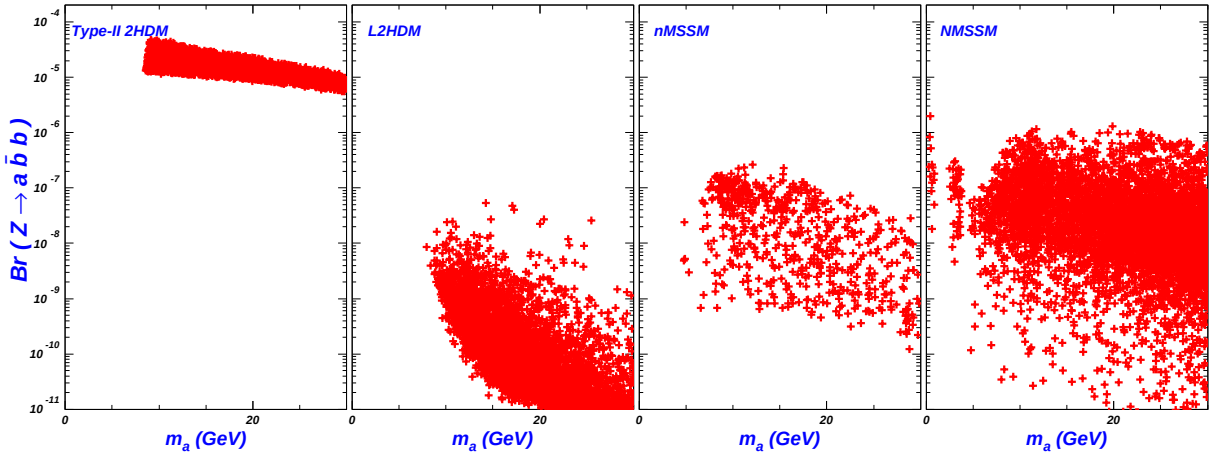

FIG. 5: Same as Fig.4, but for the branching ratio of $Z \to \bar{b}ba$ versus m_a.

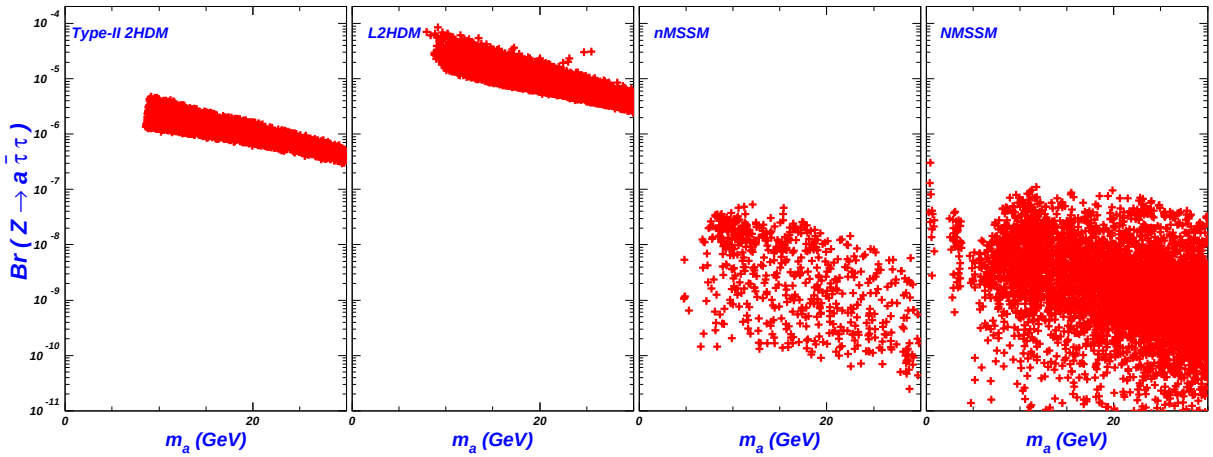

FIG. 6: Same as Fig.5, but for $Z \to \bar{\tau}\tau a$.

In Fig.4, we project the surviving samples on the $m_a - \tan\beta$ plane. This figure shows that the allowed range of $\tan\beta$ is from 8 to 20 in the Type-II 2HDM, and from 37 to 80 in the L2HDM. Just as we introduced before, the lower bounds of $\tan\beta$ come from the fact that we require the models to explain the muon anomalous moment, while the upper bound is due to we have imposed the constraint from the LEP process $e^+e^- \to \bar{b}bS \to 4b$, which have limited the upper reach of the $\bar{b}bS$ coupling for light S [33](for the dependence of $\bar{b}bS$ coupling on $\tan\beta$, see Sec. II). This figure also indicates that for the nMSSM and the NMSSM, $\tan\beta$ is upper bounded by 10. For the nMSSM, this is because large $\tan\beta$ can suppress the dark matter mass to make its annihilation difficult (see [19] and also Sec. II), but for the NMSSM, this is because we choose a light slepton mass so that large $\tan\beta$ can enhance a_μ too significantly to be experimentally unacceptable. We checked that for the slepton mass as heavy as 300GeV, $\tan\beta \geq 25$ is still allowed for the NMSSM.

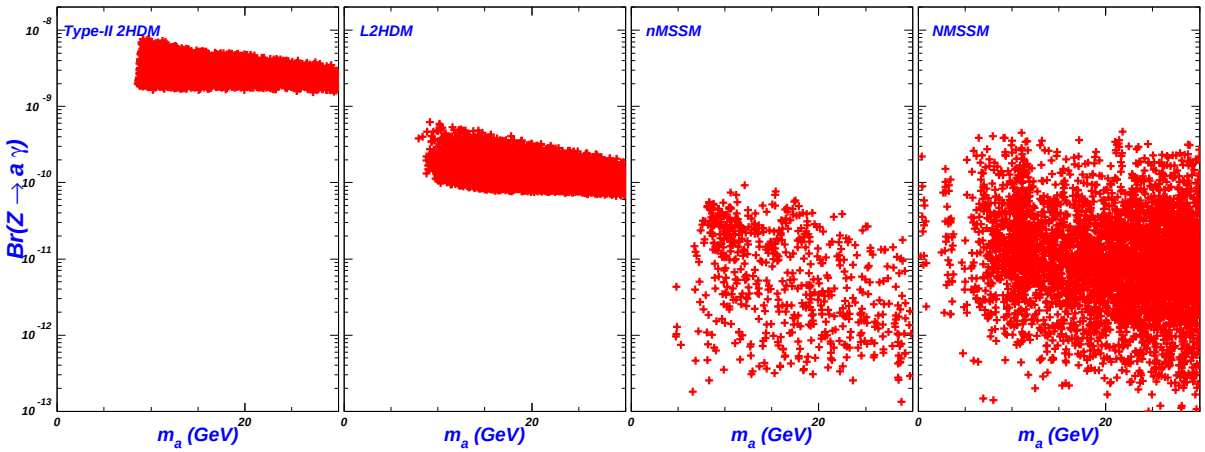

FIG. 7: Same as Fig.5, but for $Z \to a\gamma$.

In Fig.5 and Fig.6, we show the branching ratios of $Z \to \bar{b}ba$ and $Z \to \bar{\tau}\tau a$ respectively. Fig.5 indicates, among the four models, the Type-II 2HDM predicts the largest ratio for $Z \to \bar{b}ba$ with its value varying from 5×10^{-6} to 6×10^{-5}. The underlying reason is in the Type-II 2HDM, the $\bar{b}ba$ coupling is enhanced by $\tan\beta$ (see Fig.4), while in the other three model, the coupling is suppressed either by $\cot\beta$ or by the singlet component of the a. Fig.6 shows that the L2HDM predicts the largest rate for $Z \to \bar{\tau}\tau a$ with its value reaching 10^{-4} in optimum case, and for the other three models, the ratio of $Z \to \bar{\tau}\tau a$ is at least about one order smaller than that of $Z \to \bar{b}ba$. This feature can be easily understood from the $\bar{\tau}\tau a$ coupling introduced in Sect. II. Here we emphasize that, if the nature prefers a light a, $Z \to \bar{b}ba$ and/or $Z \to \bar{\tau}\tau a$ in the Type-II 2HDM and the L2HDM will be observable at the GigaZ. Then by the rates of the two decays, one can determine whether the Type-II 2HDM or the L2HDM is the right theory. On the other hand, if both decays are observed with small rates or fail to be observed, the singlet extensions of the MSSM are favored.

In Fig.7, we show the rate of $Z \to a\gamma$ as the function of m_a. This figure indicates that the branching ratio of $Z \to a\gamma$ can reach 9×10^{-9}, 6×10^{-10}, 9×10^{-11} and 4×10^{-10} for the optimal cases of the Type-II 2HDM, the L2HDM, the nMSSM and the NMSSM respectively, which implies that the decay $Z \to a\gamma$ will never be observable at the GigaZ if the studied model is chosen by nature. The reason for the smallness is, as we pointed out before, that the decay $Z \to a\gamma$ proceeds only at loop level.

Comparing the optimum cases of the Type-II 2HDM, the nMSSM and the NMSSM shown in Fig.5-7, one may find that the relation $Br_{2HDM} > Br_{NMSSM} > Br_{nMSSM}$ holds for any of the decays. This is because the decays are all induced by the Yukawa couplings with similar

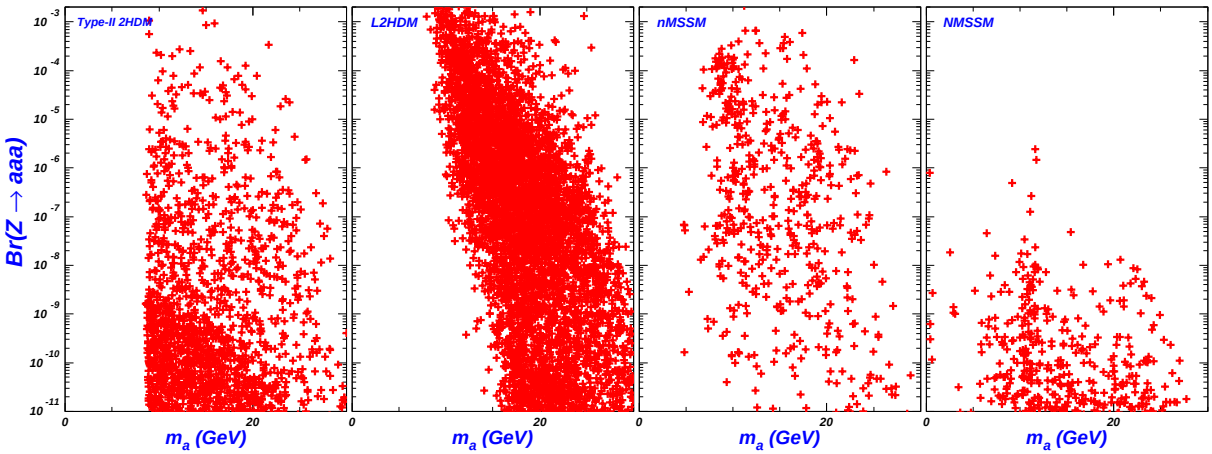

FIG. 8: Same as Fig.5, but for $Z \to aaa$.

structure for the models. In the supersymmetric models, the large singlet component of the light a is to suppress the Yukawa couplings, and the a in the nMSSM has more singlet component than that in the NMSSM.

Next we consider the decay $Z \to aaa$, which, unlike the above decays, depends on the Higgs self interactions. In Fig.8 we plot its rate as a function of m_a and this figure indicates that the $Br(Z \to aaa)$ may be the largest among the ratios of the exotic Z decays, reaching 10^{-3} in the optimum cases of the Type-II 2HDM, the L2HDM and the nMSSM. The underlying reason is, in some cases, the intermediate state h in Fig.3 (a) may be on-shell. In fact, we find this is one of the main differences between the nMSSM and the NMSSM, that is, in the nMSSM, h in Fig.3 (a) may be on-shell (corresponds to the points with large $Br(Z \to aaa)$) while in the NMSSM, this seems impossible. So we conclude that the decay $Z \to aaa$ may serve as an alternative channel to test new physics models, especially it may be used to distinguish the nMSSM from the NMSSM if the supersymmetry is found at the LHC and the $Z \to aaa$ is observed at the GigaZ with large rate.

Before we end our discussion, we note that in the NMSSM, the Higgs boson a may be lighter than 1GeV without conflicting with low energy data from Υ decays and the other observables (see Fig.4-8). In this case, a is axion-like as pointed out in [16]. We checked that, among the rare Z decays discussed in this paper, the largest branching ratio comes from $Z \to a\bar{b}b$ which can reach 1.9×10^{-6}. Since in this case, the decay product of a is highly collinear muon pair, detecting the decay $Z \to a\bar{b}b$ may need some knowledge about detectors, which is beyond our discussion.

VI. CONCLUSION

In this paper, we studied the rare Z-decays $Z \to \bar{f}fa$ ($f = b, \tau$), $Z \to a\gamma$ and $Z \to aaa$ in the Type-II 2HDM, lepton-specific 2HDM, nMSSM and NMSSM, which predict a light CP-odd Higgs boson a. In the parameter space allowed by current experiments, the branching ratio can be as large as 10^{-4} for $Z \to \bar{f}fa$, 10^{-9} for $Z \to a\gamma$ and 10^{-3} for $Z \to aaa$, which implies that the decays $Z \to \bar{f}fa$ and $Z \to aaa$ may be accessible at the GigaZ option. Since different models predict different size of branching ratios, these decays can be used to distinguish different model through the measurement of these rare decays.

Acknowledgment

This work was supported in part by HASTIT under grant No. 2009HASTIT004, by the National Natural Science Foundation of China (NNSFC) under grant Nos. 10821504, 10725526, 10635030, 10775039, 11075045 and by the Project of Knowledge Innovation Program (PKIP) of Chinese Academy of Sciences under grant No. KJCX2.YW.W10.

[1] J. A. Aguilar-Saavedra *et al.*, hep-ph/0106315.

[2] For some reviews, see, e.g., M. A. Perez, G. Tavares-Velasco and J. J. Toscano, Int. J. Mod. Phys. A **19**, 159 (2004); J. M. Yang, arXiv:1006.2594.

[3] J. I. Illana, M. Masip, Phys. Rev. D **67**, 035004 (2003); J. Cao, Z. Xiong, J. M. Yang, Eur. Phys. J. C **32**, 245 (2004).

[4] D. Atwood *et al.*, Phys. Rev. D **66**, 093005 (2002).

[5] J. Kalinowski, and S. Pokorski, Phys. Lett. B **219**, 116 (1989); A. Djouadi, P. M. Zerwas and J. Zunft, Phys. Lett. B **259**, 175 (1991); A. Djouadi, J. Kalinowski, and P. M. Zerwas, Z. Phys. C **54**, 255 (1992).

[6] M. Krawczyk, *et al.*, Eur. Phys. J. C **19**, 463 (2001); Eur. Phys. J. C **8**, 495 (1999).

[7] J. F. Gunion, G. Gamberini and S. F. Novaes, Phys. Rev. D **38**, 3481 (1988); Thomas J. Weiler and Tzu-Chiang Yuan, Nucl. Phys. B **318**, 337 (1989); A. Djouadi, *et al.*, Eur. Phys. J. C **1**, 163 (1998)[hep-ph/9701342].

[8] D. Chang and W. Y. Keung, Phys. Rev. Lett. **77**, 3732 (1996).

[9] E. Keith and E. Ma, Phys. Rev. D **57**, 2017 (1998); M. A. Perez, G. Tavares-Velasco and J. J. Toscano, Int. J. Mod. Phys. A **19**, 159 (2004).

[10] F. Larios, G. Tavares-Velasco and C. P. Yuan, Phys. Rev. D **64**, 055004 (2001); Phys. Rev. D **66**, 075006 (2002).

[11] A. Djouadi, *et al.*, Eur. Phys. J. C **10**, 27 (1999) [hep-ph/9903229].

[12] For a detailed introduction of the NMSSM, see F. Franke and H. Fraas, Int. J. Mod. Phys. A **12** (1997) 479; for a recent review of the NMSSM, see for example, U. Ellwanger, C. Hugonie, and A. M. Teixeira, arXiv: 0910.1785.

[13] See, e.g., J. R. Ellis, J. F. Gunion, H. E. Haber, L. Roszkowski and F. Zwirner, Phys. Rev. D **39** (1989) 844; M. Drees, Int. J. Mod. Phys. A **4** (1989) 3635; U. Ellwanger, M. Rausch de Traubenberg and C. A. Savoy, Phys. Lett. B **315** (1993) 331; Nucl. Phys. B **492** (1997) 21; D.J. Miller, R. Nevzorov, P.M. Zerwas, Nucl. Phys. B **681**, 3 (2004).

[14] C. Panagiotakopoulos, K. Tamvakis, Phys. Lett. B **446**, 224 (1999); Phys. Lett. B **469**, 145 (1999); C. Panagiotakopoulos, A. Pilaftsis, Phys. Rev. D **63**, 055003 (2001); A. Dedes, *et al.*, Phys. Rev. D **63**, 055009 (2001); A. Menon, *et al.*, Phys. Rev. D **70**, 035005 (2004); V. Barger, *et al.*, Phys. Lett. B **630**, 85 (2005). C. Balazs, *et al.*, JHEP **0706**, 066 (2007).

[15] B. A. Dobrescu, K. T. Matchev, JHEP **0009**, 031 (2000); A. Arhrib, K. Cheung, T. J. Hou, K. W. Song, hep-ph/0611211; JHEP **0703**, 073 (2007); X. G. He, J. Tandean, and G. Valencia, Phys. Rev. Lett. **98**, 081802 (2007); JHEP **0806**, 002 (2008); F. Domingo *et al.*, JHEP **0901**, 061 (2009); Gudrun Hiller, Phys. Rev. D **70**, 034018 (2004); R. Dermisek, and John F. Gunion, Phys. Rev. D **75**, 075019 (2007); Phys. Rev. D **79**, 055014 (2009); Phys. Rev. D **81**, 055001 (2010); R. Dermisek, John F. Gunion, and B. McElrath, Phys. Rev. D **76**, 051105 (2007); Z. Heng, *et al.*, Phys. Rev. D **77**, 095012 (2008); A. Belyaev *et al.*, Phys. Rev. D **81**, 075021 (2010); D. Das and U. Ellwanger, arXiv:1007.1151 [hep-ph].

[16] S. Andreas, O. Lebedev, S. Ramos-Sanchez and A. Ringwald, arXiv:1005.3978 [hep-ph].

[17] J. F. Gunion, JHEP **0908**, 032 (2009); R. Dermisek and J. F. Gunion, Phys. Rev. D **81**, 075003 (2010).

[18] R. Dermisek and J. F. Gunion, Phys. Rev. Lett. **95**, 041801 (2005); Phys. Rev. D **73**, 111701 (2006).

[19] J. Cao, H. E. Logan, J. M. Yang, Phys. Rev. D **79**, 091701 (2009).

[20] J. Cao, P. Wan, L. Wu, J. M. Yang, Phys. Rev. D **80**, 071701 (2009).

[21] J. F. Gunion and H. E. Haber, Phys. Rev. D **67**, 075019 (2003).

[22] R. M. Barnett, *et al.*, Phys. Lett. B **136**, 191 (1984); R. M. Barnett, G. Senjanovic and D. Wyler, Phys. Rev. D **30**, 1529 (1984); Y. Grossman, Nucl. Phys. B **426**, 355 (1994).

[23] H. S. Goh, L. J. Hall and P. Kumar, JHEP **0905**, 097 (2009); A. G. Akeroyd and W. J. Stirling, Nucl. Phys. B **447**, 3 (1995); A. G. Akeroyd, Phys. Lett. B **377**, 95 (1996); H. E. Logan and D. MacLennan, Phys. Rev. D **79**, 115022 (2009); M. Aoki, *et al.*, arXiv:0902.4665 [hep-ph].

[24] V. Barger, P. Langacker, H. S. Lee and G. Shaughnessy, Phys. Rev. D **73**, 115010 (2006).

[25] S. Hesselbach, *et. al.*, arXiv:0810.0511v2 [hep-ph].

[26] A. G. Akeroyd, A. Arhrib and E. M. Naimi, Phys. Lett. B **490**, 119 (2000).

[27] R. Barate *et al.*, Phys. Lett. B **565** (2003) 61.

[28] OPAL collaboration, Eur. Phys. J. C **27** (2003) 483.

[29] ALEPH Collaboration, JHEP **1005**, 049 (2010)[arXiv:1003.0705].

[30] DELPHI Collaboration, Eur. Phys. J. C **38** (2004) 1.

[31] D. Buskulic, *et al.*, Phys. Lett. B **313** (1993) 312; G. Abbiendi, *et al.*, Eur. Phys. J. C **27** (2003) 311.

[32] K. Mönig, DELPHI 97-174 PHYS 748.

[33] J.B. de Vivie and P. Janot [ALEPH Collaboration], PA13-027 contribution to the International Conference on High Energy Physics, Warsaw, Poland, 25–31 July 1996; J. Kurowska, O. Grajek and P. Zalewski [DELPHI Collaboration], CERN-OPEN-99-385.

[34] [ALEPH Collaboration and DELPHI Collaboration and L3 Collaboration], Phys. Rept. **427**, 257 (2006).

[35] J. Cao and J. M. Yang, JHEP **0812**, 006 (2008).

[36] M. Krawczyk and D. Temes, Eur. Phys. J. C **44**, 435 (2005).

[37] G. Altarelli and R. Barbieri, Phys. Lett. B **253**, 161 (1991); M. E. Peskin, T. Takeuchi, Phys. Rev. D **46**, 381 (1992).

[38] C. Amsler, *et al.*, (Particle Data Group), Phys. Lett. B **667**, 1 (2008).

[39] O. Deschamps, S. Descotes-Genon, S. Monteil, V. Niess, S. T'Jampens and V. Tisserand, arXiv:0907.5135 [hep-ph].

[40] S. Su and B. Thomas, Phys. Rev. D **79**, 095014 (2009).

[41] G. Abbiendi, *et al.*, Eur. Phys. J. C **32**, 453 (2004).

[42] M. Davier, *et al.*, Eur. Phys. J. C **66**, 1 (2010).

[43] K. Cheung, *et al.*, Phys. Rev. D **64**, 111301 (2001).

[44] K. Cheung and O. C. W. Kong, Phys. Rev. D **68**, 053003 (2003).

[45] T. Besmer, C. Greub, T.Hurth, Nucl. Phys. B **609**, 359 (2001); F. Borzumati, *et al.*, Phys. Rev. D **62**, 075005(2000).

[46] J. Cao, K. i. Hikasa, W. Wang, J. M. Yang and L. X. Yu, Phys. Rev. D **82**, 051701 (2010) [arXiv:1006.4811 [hep-ph]].

[47] J. F. Gunion, *et. al.*, Phys. Rev. D **73**, 015011 (2006).

[48] S. P. Martin and J. D. Wells, Phys. Rev. D **64**, 035003 (2001).

[49] J. Abdallah *et al.*, Eur. Phys. J. C **31**, 421 (2004); G. Abbiendi *et al.*, Eur. Phys. J. C **35**, 1 (2004).

[50] J. Dunkley *et al.* [WMAP Collaboration], Astrophys. J. Suppl. **180**, 306 (2009) [arXiv:0803.0586 [astro-ph]].

[51] U. Ellwanger *et al.*, JHEP **02**, 066 (2005).

[52] G. Belanger, F. Boudjema, A. Pukhov and A. Semenov, Comput. Phys. Commun. **174**, 577 (2006); Comput. Phys. Commun. **176**, 367 (2007).

[53] G. Belanger, F. Boudjema, C. Hugonie, A. Pukhov and A. Semenov, JCAP **0509**, 001 (2005).